Hindawi Publishing Corporation
International Journal of Electrochemistry
Volume 2014, Article ID 932654, 16 pages
http://dx.doi.org/10.1155/2014/932654

Research Article

Role of Indium Alloying with Lead as a Means to Reduce the Passivation Phenomena in Lead/Acid Batteries

Abdel-Rahman El-Sayed, Hossnia S. Mohran, and Hoda Abdel Shafy Shilkamy

Department of Chemistry, Faculty of Science, Sohag University, Sohag 82524, Egypt

Correspondence should be addressed to Abdel-Rahman El-Sayed; elsayed777@yahoo.com

Received 28 June 2014; Revised 27 July 2014; Accepted 31 July 2014; Published 23 September 2014

Academic Editor: Sheng S. Zhang

The influence of indium content on the anodic behaviour of Pb-In alloys in 4 M H_2SO_4 solution is investigated by potentiodynamic, potentiostatic, chronopotentiometric, and cyclic voltammetric techniques. The composition and microstructure of the corrosion layer on Pb-In alloys are characterized by X-ray diffraction (XRD), energy-dispersive X-ray spectroscopy analysis (EDX), and scanning electron microscopy (SEM). The potentiodynamic and chronopotentiometric curves show that the anodic behavior of all investigated electrodes exhibits active/passive transition. The active dissolution (except for alloy I) and passive currents increase with increasing both In content and temperature. This indicates that the conductivity of the anodic film on Pb-In alloy is enhanced. This study exhibits that indium catalyses the oxidation of Pb (II) to Pb (IV) and facilitates the formation of a more highly conductive corrosion layer on lead. Alloy I (0.5% In) exhibits that the corrosion rate is lower, while the passive current is higher than that of Pb. XRD, EDX, and SEM results reveal that the formation of both $PbSO_4$ and PbO on the surface decreases gradually with increasing In level in the alloy and completely disappear at higher In content (15% In). Therefore, recharge of the battery will be improved due to indium addition to Pb.

1. Introduction

Generally, lead and lead alloy were used as the grid material of the lead acid battery, due to their good anticorrosion performance in H_2SO_4 solution. The use of pure Pb gives rise to strong oxide passive layer formation at the grid/active material interface [1]. This oxide layer is highly stable in the presence of H_2SO_4 solution. The insulating passive film reduces the anode dissolution, thereby increasing the active life of the battery [2]. However, this also has an undesirable effect of increasing the impedance of the anode after storage for a certain period of time. The increase in the resistance reduces both the reversibility and charging efficiency during subsequent cycles [3].

Passivation of lead and lead alloys is believed to occur by the formation of highly resistive α-PbO at the interface between the grid and the active material during the oxidation of lead to lead dioxide, which passivate the electrical contact over the boundary layer [4–9]. α-PbO is formed under the lead sulphate layer where the local pH value is close to 9 due to the semipermeable properties of the lead sulphate layer, allowing a flux of H^+, OH^-, and water species, while hindering SO_4^{2-} and HSO_4^- ions [9]. The solution of this problem is the addition of tin as alloying element to lead. Studies indicate that tin alloying with Pb makes the PbO layer thinner [10, 11], promotes the oxidation of tet-PbO or α-PbO to PbO_n ($1 < n < 2$), and lowers the potential at which this reaction initiates [12, 13]. Two comprehensive reviews covering the literature about the role of tin as an alloying element to eliminate problems of passivation have been presented by Nelson and Wisdom [3] and by Culpin et al. [2]. Thus, the presence of tin in the oxide layer has been confirmed. Tin has been shown to alleviate the passivation problem [11, 13]. Fundamental research has been performed to elucidate the action of tin alloying with Pb on the electronic properties of the PbO layer and to determine the optimum level of tin in the alloy. The nature of the passivation layer and the conditions of its formation have been well defined. The generally accepted view is that the passivation layer, namely, α-PbO, acts as a semiconductor or an electrical insulator. The effect of tin on grid passivation has been known a long time ago [2], but previous studies on the effect of tin on the

Table 1: Chemical composition (weight percent) of alloys.

Alloy number	I	II	III	IV	V
Composition	$Pb_{99.5}In_{0.5}$	$Pb_{99}In_{1.0}$	$Pb_{95}In_{5.0}$	$Pb_{90}In_{10}$	$Pb_{85}In_{15}$

passive film formation were stimulated by the investigations of Pavlov et al. [13]. The electron conductivity of lead oxide increases strongly with the value of n, and PbO_2 is very electron conductive. In this way, Sn increases the oxidation rate of PbO to PbO_n and thus eliminates the formation of α-PbO. However, the problem in using Pb-Sn alloys as grid material in the lead acid battery is the observed decrease in conductivity for long periods of time. This behavior was explained by the slow dissolution of tin oxide in H_2SO_4 [14]. Indium alloying with lead suppresses the growth of PbO phase. Accordingly, the corrosion of Pb into PbO can be controlled or can be prevented by incorporating indium in the lead. Consequently, the conductivity of the passivation layer on Pb-In alloy is improved. Therefore, Pb-In alloys may be proposed to replace Pb-Sn alloys as grid materials. In the present investigation, the anodic oxidation of Pb-In alloys in 4 M H_2SO_4 solution was studied as a function of In content. The oxidation behavior was studied by means of potentiodynamic, potentiostatic, chronopotentiometric, and cyclic voltammetric measurements. The passive film formed on the surface of electrodes at various potentials was characterized using X-ray diffraction, EDX, and scanning electron microscopy (SEM).

2. Experimental Procedure

2.1. Materials and Solutions. A stock solution of 4 M H_2SO_4 acid (the acid concentration used in the lead/acid battery) was prepared by dilution of the calculated volume of A.R. grade acid. Pb and In of high purity (99.999%; Johnson Matthey Chemicals Ltd.) were used to prepare Pb-In alloys as disk electrodes ($A = 0.196\,cm^2$) in a Gallenkamp muffle furnace using evacuated closed silica tubes at 500°C for 24 h. The melts were shaken every 6 h to ensure the homogeneity of melting alloy and finally the melts were quenched in an ice as previously discussed [15]. Five Pb-In alloys were prepared with the composition shown in Table 1. The prepared alloys were analyzed using X-ray photoelectron spectroscopy. For the alloys, the percentage of Pb and In was found in accordance with the percentage of mixing Pb and In. The microstructure and composition of the studied alloys were investigated using X-ray diffraction and SEM micrographs. It was found that solid solution phase is formed, and the composition is homogeneous.

2.2. Electrochemical Measurements. The measurements were performed on planar disk electrode embedded in an Araldite holder. Prior to each measurement the electrodes were polished with sequacious grades of emery paper, degreased in pure ethanol, and washed in running bidistilled water before being inserted in the polarization cell. A conventional three-electrode system was used; the counter electrode was a Pt sheet with an area of 1 cm × 2 cm. The reference electrode was a saturated calomel electrode (SCE) to which all potentials are referred and connected via a Luggin's capillary. The cell description was given elsewhere [16]. To remove any surface contamination and air formed oxide, the working electrode was kept at −1.5 V (SCE) for 5 min in the tested solution, disconnected, and shaken free of adsorbed hydrogen bubbles. Then, each electrode was left in the solution (30 min) to reach steady state potential ($E_{o.c.p}$) before the anodic polarization measurements. Potentiostat/Galvanostat (EG&G Model 273) connected with a personal computer (IBM Model 30) was used for the measurements. Software 342 C and version 270 (used for cyclic voltammetric measurements) supplied from Princeton Applied Research were used for all the electrochemical measurements.

In the case of potentiodynamic measurements, the potential was altered automatically in the positive direction from the open circuit potential ($E_{o.c.p}$) up to +1.5 V versus SCE and at scan rate 1 mV s^{-1}. In some potentiostatic experiments, the anodic potential was fixed at required constant value and the variation of current density was recorded as a function of time (current density-time transients). Details of the experimental procedure have been described elsewhere [17]. In chronopotentiometry potential/time transients, a constant current density is applied on the anode and the variation in potential was recorded as a function of time. Cyclic voltammograms of the pure Pb and Pb-In alloys as electrodes in H_2SO_4 solution and potential region between −1.2 and 1.5 V were obtained at a constant sweep rate (10 m V s^{-1}).

2.3. Surface Characterization. X-ray diffraction of the corrosion products formed on the surfaces of Pb and Pb-In alloys was carried out using the X-ray diffraction technique (Bruker AXS-D8 Advanced diffractometer) using Cu-Kα radiation ($\lambda = 1.5418\,A^\circ$). The composition and morphology of corrosion products formed on the surfaces of electrodes were examined using energy-dispersive X-ray spectroscopy analysis (EDX) conducted with scanning electron microscope (SEM) (SEM-EDX) (JEOL, model 5300). Each experiment was performed with freshly prepared solution and clean set of each electrode. Measurements were conducted at 20, 30, 40, and 50 ± 0.5°C for each investigated electrode. For this purpose ultrathermostat model Frigiter 600 382 (SELECTA) was used.

3. Results and Discussion

3.1. Potentiodynamic Polarization Curves

3.1.1. Effect of Indium Content. Figure 1 shows a comparison between the potentiodynamic polarization curves for pure lead and Pb-0.5 In alloy in 4 M H_2SO_4 solution. The polarization curves were swept from steady state of open circuit potential ($E_{o.c.p}$) up to +1500 mV (SCE) at scan rate 1 mV s^{-1}

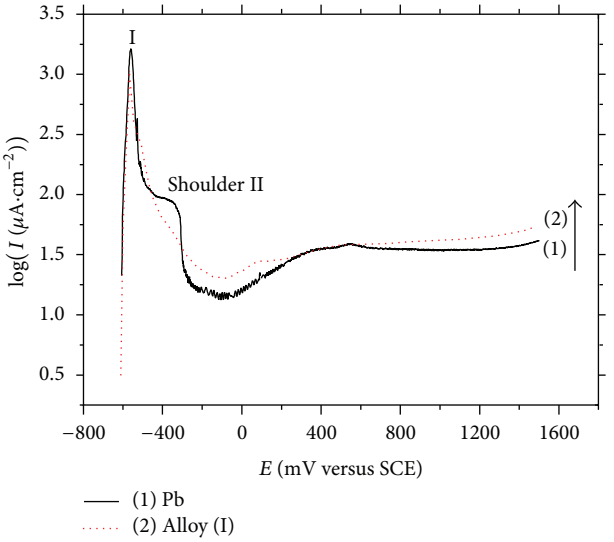

Figure 1: Potentiodynamic anodic polarization curves for Pb and Pb-0.5 In alloy in 4 M H_2SO_4 solution and at 20°C.

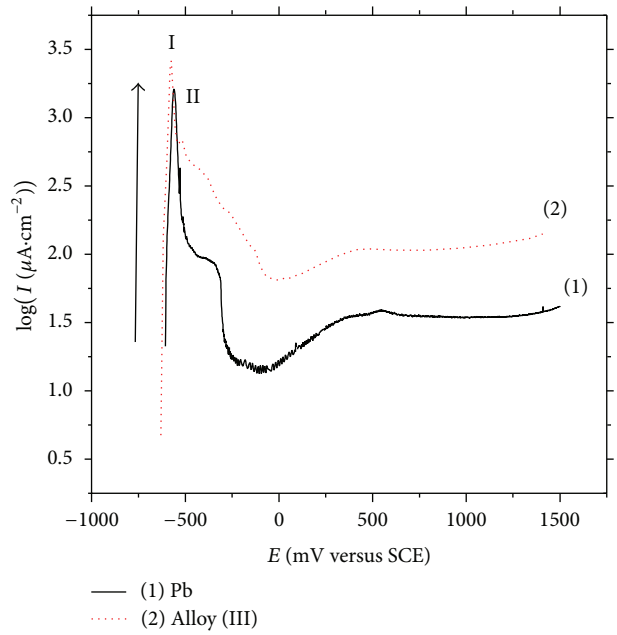

Figure 2: Potentiodynamic anodic polarization curves for Pb and Pb-5 In alloy in 4 M H_2SO_4 solution and at 20°C.

and 20°C. The data reveal that the anodic excursion exhibits active-passive transition of both lead and its investigated alloy. The active dissolution region involves a well-defined one anodic peak I and shoulder II of the pure lead, followed by a passive region, which extends up to +1500 mV (SCE) with almost constant current density ($I_{pass.}$). The anodic peak I is located at about −565 mV (SCE), which can be associated with the active dissolution of Pb to Pb (II) species according to the reaction [18]

$$Pb \longrightarrow Pb^{2+} + 2e \quad (1)$$

$$Pb^{2+} + SO_4{}^{2-} \longrightarrow PbSO_4 \quad (2)$$

where Pb^{2+} and $SO_4{}^{2-}$ ions exceed the solubility product of $PbSO_4$; it precipitates on the electrode surface and thus the current drops, suggesting the onset of the primary passivation at a potential comparable with the equilibrium potential of the system $Pb/PbSO_4$. On the other hand, the shoulder II observed at about −366 mV (SCE) is related to electrooxidation of Pb to PbO. PbO is insoluble and precipitates [18] on lead surface, giving rise to a passivation film. At potentials between −200 and +618 mV (SCE) the current density starts to slightly increase again, which may be due to the partial dissolution of $PbSO_4$ in H_2SO_4 solution in this region. A partial stabilization on current density is observed between potentials +618 and +1400 mV (SCE). This indicates the precipitation and dissolution mechanisms of $PbSO_4$ particles, as also verified in previous study [19].

The curve of potentiodynamic anodic polarization of alloy I (0.5% In) in the same acid solution under the same conditions exhibits similar behaviour to that observed in the case of pure Pb (except that shoulder II, disappeared). However, it is observed that the anodic peak current is decreased compared with that of pure lead. This behaviour suggests that addition of minor In to Pb plays an important role in decreasing peak current. Therefore, the decrease of anodic corrosion current of the mentioned alloy (0.5% In) under the same conditions improves its stability against corrosion [15]. This behaviour indicates a beneficial effect of minor In content in the alloy. It may be that the In atoms in the lead alloy during lead dissolution tend to remain on the surface. They also appear to mostly locate at the edges of the steps. Since dissolution of crystalline structures typically proceeds layer by layer along the steps, thus it may have an effect of blocking the sites for the dissolution reaction [20].

It is interesting to observe that shoulder II for alloy I seems to have disappeared. This behaviour can be attributed to the presence of In with lead, retarding the formation of PbO on the surface. Mukhopadhyay et al. [21] showed that α-PbO gradually decreased with the increase in indium concentration in Pb-In alloy. This behaviour supported that In passivates the lead from its oxidation to PbO. Accordingly, the growth of Pb (II) in the corrosion film was inhibited by adding indium. On the other hand, the current density of the passive region ($I_{pass.}$) is higher in the case of Pb-0.5% In alloy than that of pure lead. These results suggest that the alloy surface is less protected, due to the formation of another type of semiconducting oxide but less resistant than PbO [14].

Figures 2 and 3 represent a comparison between the potentiodynamic polarization curves of Pb with both alloys III (5% In) and V (15% In) at 20°C in the examined acid solution. These curves reveal that the addition of indium (from 1 to 15% In) to Pb has the influence of increasing peak current compared with that of Pb. The peak current gradually increases with increasing In content. This behaviour exhibits very interesting results that indium content in the alloys (II to V) plays an important role in the active dissolution of Pb in H_2SO_4 solution. The curves of alloys II and III are similar to that of alloy I. This shows that the curves have nearly the same

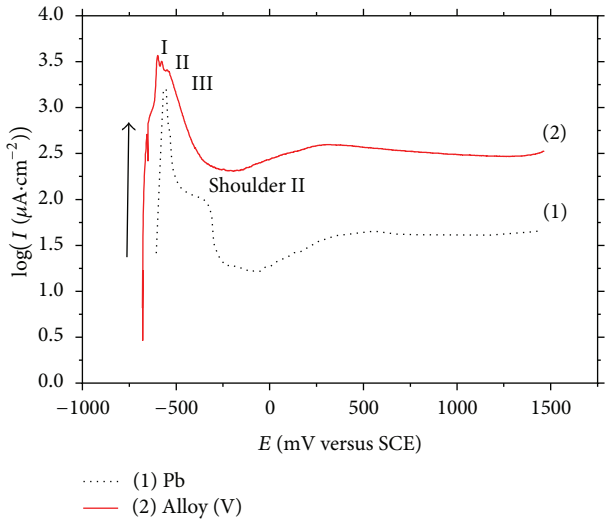

Figure 3: Potentiodynamic anodic polarization curves for Pb and Pb-15 In alloy in 4 M H_2SO_4 solution and at 20°C.

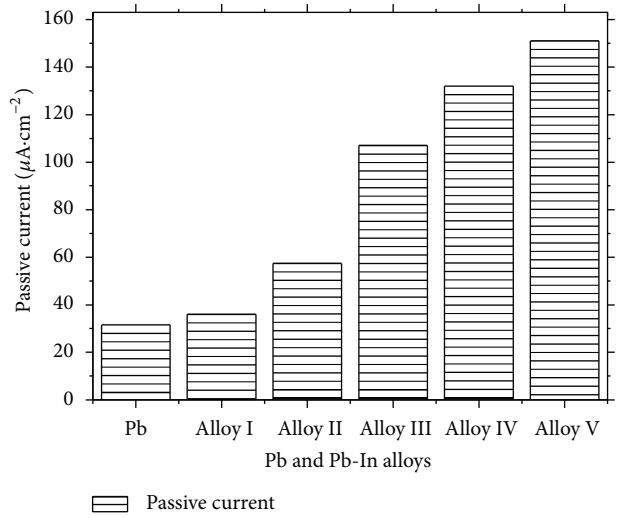

Figure 4: Effect of indium alloying with Pb on passivation current density at +1.2 V versus SCE and 20°C.

general feature. They are characterized by the appearance of one peak only. Therefore, the observed peaks of alloys (I to III) may be attributed to the formation of mixed oxides of both lead and indium. On the other hand, it is observed that the values of the anodic peak current (alloys II and III) increase with increasing In content compared with that of pure lead. This value is the lowest in the case of alloy I (0.5% In) compared with those of Pb and another alloys, containing higher In content. Alloys IV and V exhibit different behaviour compared to that of the first three alloys. However, the data of alloy IV (not represented here) show two peaks: the first at a potential of about −594 mV and the second at −580 mV. It is observed that the current of peak I is higher than that of peak II. This peak II may be attributed to the formation of $In(OH)_3$. The curve of alloy V (Figure 3) shows three peaks: the first at a potential of about −601 mV, the second at −583 mV, and the third at −541 mV. The three peaks are very close to each other. However, the data reveal that the value of the anodic current of peak I is higher than those of peaks II and III. The observed peak I can be attributed to the oxidation of Pb to $PbSO_4$, which may be oxidized to β-PbO_2 according to the following reaction [22]:

$$PbSO_4 + 2H_2O \longrightarrow \beta\text{-}PbO_2 + H_2SO_4 + 2H^+ + 2e \quad (3)$$

Peaks II and III may be attributed to the formation of $In(OH)_3$ and In_2O_3, respectively, due to the high In content in the alloy V. This is confirmed by X-ray diffraction and SEM.

Figure 4 shows the effect of indium alloying with Pb on passivation current of the investigated electrodes at +1200 mV (SCE) and 20°C. In general, the passivation current increases gradually with increasing In content. This indicates that the addition of In enhances conductivity of the corrosion layer. The effect of In on the corrosion properties of Pb-In alloy can be discussed in two folds [23]: conductivity and ion transportation. Transportation of ions and electrons in the passive layer are the two most important processes to determine the corrosion rate of the alloys and the slower process between these two could be the controlling step of the corrosion reaction. It has been found that In can improve the conductivity of the passive film on the alloy surface by promoting the formation of β-PbO_2, having resistance values lower than those of both $PbSO_4$ and PbO [11]. When In was present in the alloy, more indium oxide was incorporated in the lead oxide, leading to a great increase of the electronic conductivity of the passive layer [14]. It is generally observed that with the incorporation of indium in the alloys, formation of PbO is impeded and the thickness of the passivation layer decreases as the indium level increases. The general proposed mechanism is the catalytic oxidation of PbO to β-PbO_2 as reported earlier [24]. Another suggested mechanism [25] is disproportionation reaction as the following:

$$In_2O + 2PbO \longrightarrow In_2O_3 + 2Pb \quad (4)$$

and/or

$$2\,In + 3PbO \longrightarrow In_2O_3 + 3Pb \quad (5)$$

Both Pb and In_2O_3 are very conductive. This study exhibits that indium ions have an acidic character and inhibit the nucleation and the growth of PbO which is stable only in alkaline medium [24]. Therefore, indium alloying with lead increases the amount of nonstoichiometric oxide and facilitates the formation of a more highly conductive corrosion layer on lead.

3.1.2. Effect of Temperature on the Anodic Polarization. Figure 5 shows the potentiodynamic polarization curves for pure Pb anode in the investigated acid solution at different temperatures (20–50°C). It is observed that the peak and passivation currents increase, while their corresponding peak potentials (peak I and shoulder II) shift to more positive direction as an increase in temperature. In addition, the observed shoulder II becomes more prominent at higher

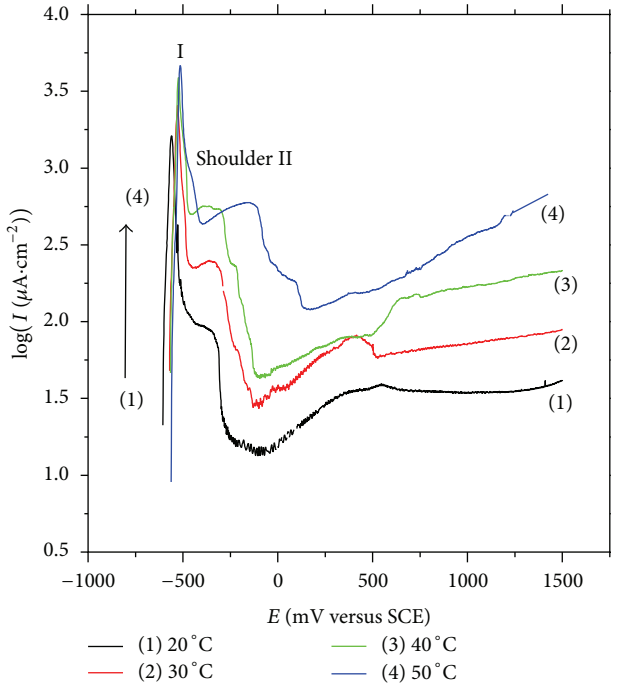

Figure 5: Potentiodynamic anodic polarization curves of Pb in 4 M H_2SO_4 solution at different temperatures.

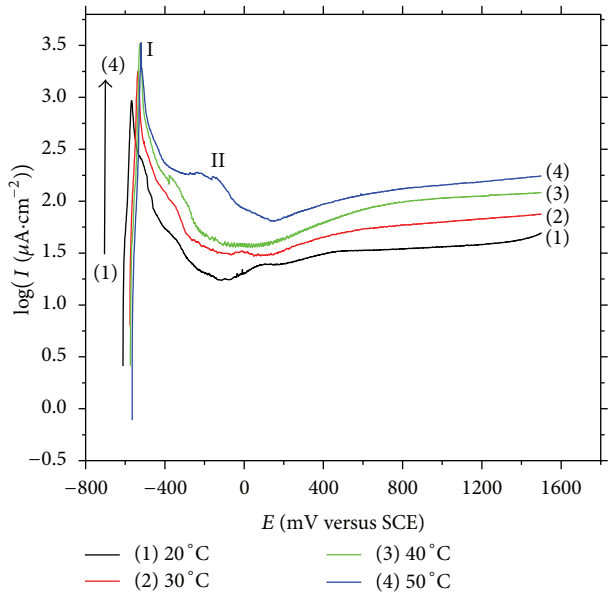

Figure 6: Potentiodynamic anodic polarization curves of alloy I in 4 M H_2SO_4 solution at different temperatures.

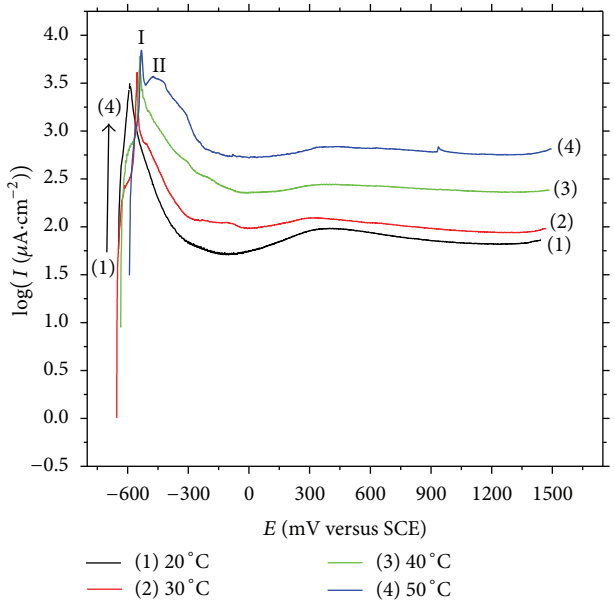

Figure 7: Potentiodynamic anodic polarization curves of alloy IV in 4 M H_2SO_4 solution at different temperatures.

temperatures. This indicates that the passivating oxide film on the surface of pure lead is able to sustain high current density by the removal of lead in the form of more soluble ions. This leads to an increase in the peak current and to a positive shift in the peak potentials with a simultaneous delay in the passivation and consequently an increase in the corrosion rate [26]. This fact implies that most Pb dissolves into the solution as $PbSO_4$ and the passivation oxide film must be quite thin [27]. The data exhibit that the current density of the passive region of pure lead gradually increases at the highest temperature (50°C) compared with those at lower temperatures (20–40°C). This behaviour can be interpreted on the basis that the oxide film formed on the Pb surface at more positive potential tends to be partially soluble at higher temperature. This behaviour could be ascribed to the effect of the chemical dissolution of the passive film in acid solution.

Figure 6 represents potentiodynamic anodic curves of alloy I (0.5% In) in the studied acid solution at different temperatures. The present data display that with increasing temperature, the peak current is also increased, while its corresponding peak slightly shifted to more positive potential. This behaviour is similar to that observed of pure lead. However, it is interesting to observe that the shoulder II appears again at higher temperature only (50°C). This behaviour can be explained in terms of competition between the formation of PbO and its chemical dissolution [28]. This phenomenon can be attributed to that the high temperature facilitates the oxidation of Pb to PbO. The data obtained for alloys II and III are similar to those of alloy I. This exhibits that the curves have nearly the same general feature. They are characterized by the appearance of one peak only (except at 50°C shoulder II is also observed).

Alloys IV and V (Figures 7 and 8) exhibit different behaviour compared to that observed in the first three alloys. As mentioned above, the curves show two peaks for alloy IV and three for alloy V. However, the data reveal that the anodic current of peak III is small compared to those of peaks I and II. On the other hand, it is observed that peak III decreases gradually because of an increase in temperature and completely disappeared at higher temperature, in addition to peak II which also becomes very small (Figure 8). This

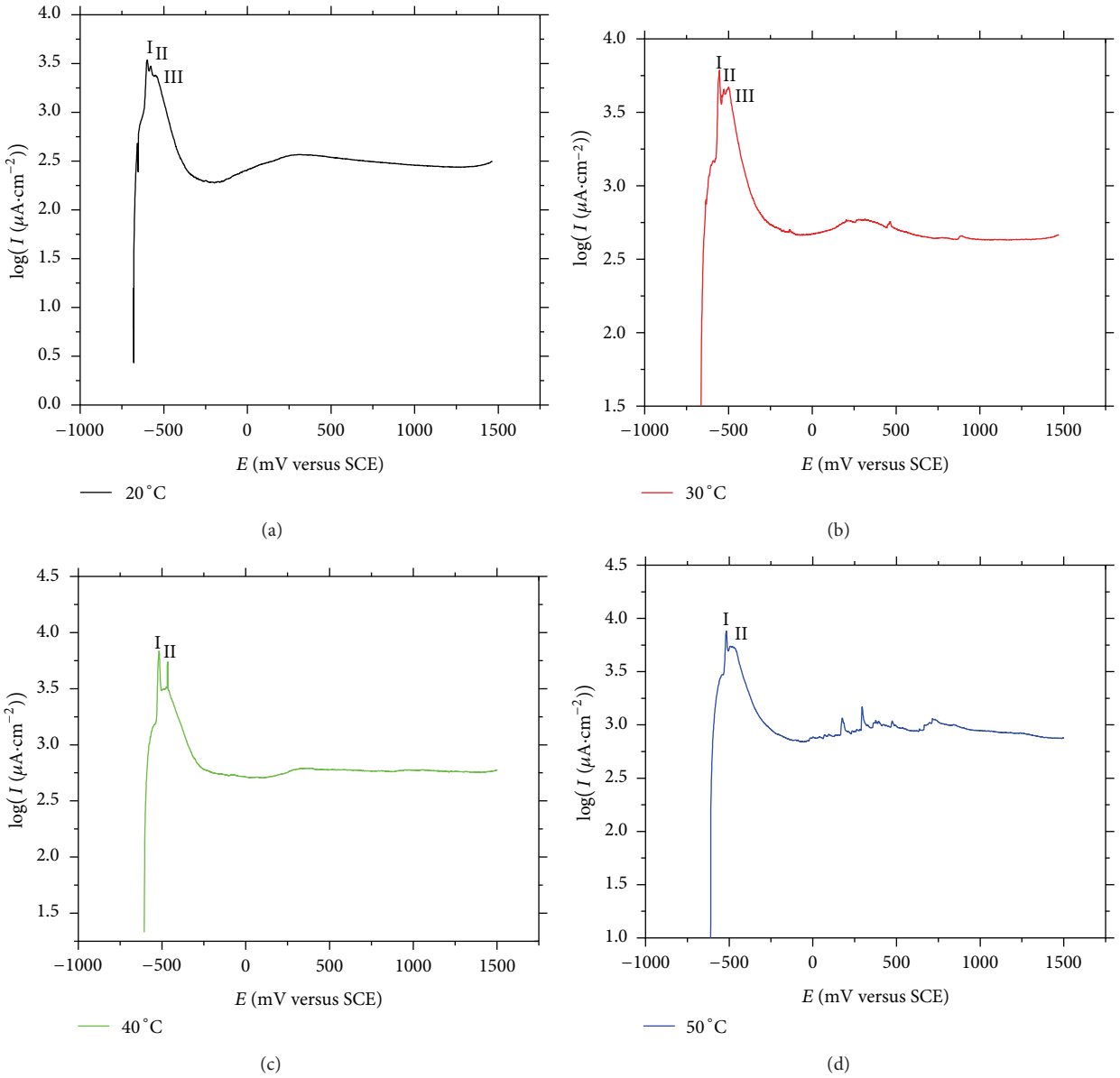

FIGURE 8: Potentiodynamic anodic polarization curves of alloy V in 4 M H_2SO_4 solution at different temperatures. (a) 20°C, (b) 30°C, (c) 40°C, and (d) 50°C.

indicates that In_2O_3, which may be formed at peak III, dissolves in acid solution particularly at high temperature. This behaviour may be due to the presence of In as a high content in the alloy V, enhancing the dissolution current and leading to an increase in the peak and passivation currents. This behaviour confirms that the tendency of the mentioned alloys toward passivity decreases with increasing indium content. These results suggest that the alloy surface is less protected most probably by the formation of more porous anodically formed films of mixed oxides from both Pb and In and the significant dissolving power of the studied acid on those oxides [28].

The log values of both peak current ($I_{\text{peak.}}$) and passivation current (I_p) for various temperatures were plotted versus $1/T$ (K^{-1}) in Figures 9 and 10. The apparent activation energy (E_a) values for the corrosion and passivation currents of pure lead and its studied alloys are determined from the slope of $\log I_{\text{peak.}}$ or $\log I_p$, respectively, versus $1/T$ plots, which are given in Table 2. The data in Table 2 show that the (E_a) value of Pb-0.5% In alloy is higher than that of pure lead. This behaviour probably is due to the higher energy barrier which is attributed to the hindrance of dissolution process at minor In content in the alloy [26]. However, the activation energy value (E_a) starts to decrease (at more than 0.5% In) with increasing In content and reaches its minimum value in the case of alloy V. This observed lower energy barrier would be attributed to the promotion of the dissolution process by increasing In content in the case of

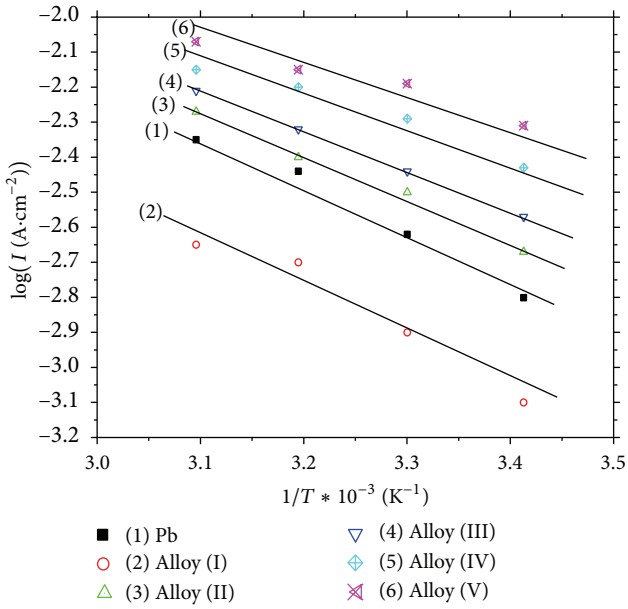

Figure 9: Arrhenius plots for Pb and its investigated alloys corrosion in 4 M M H_2SO_4 solution at peak (I).

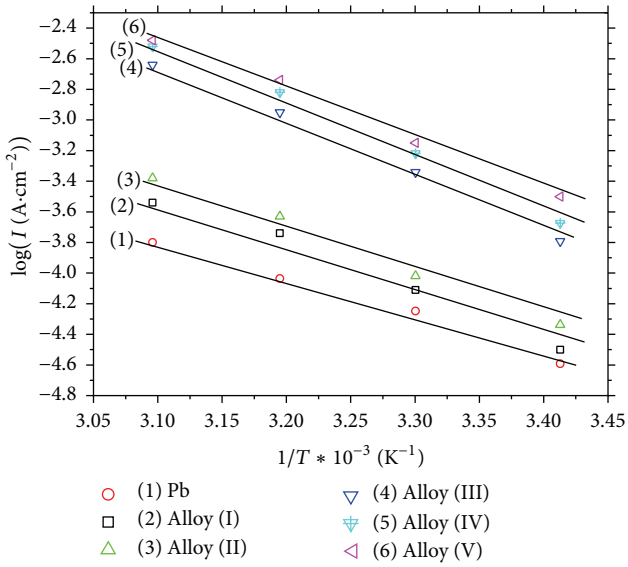

Figure 10: Arrhenius plots for Pb and its investigated alloys corrosion in 4 M H_2SO_4 solution at passive region.

alloys II-V [28]. These obtained values of E_a support the trend of corrosion rate (peak current) which is obtained for Pb and its studied alloys as mentioned before. A similar trend (except for alloy I) is observed for Pb and its alloys at passive potential (+1200 mV versus SCE). The data show that the (E_a) value decreases gradually with increasing In content and reaches its minimum value in the case of alloy V. This indicates that the passive film formed on Pb-In alloys with indium content exhibits good electronic conductivity, while the passive film formed on pure lead is more resistive [29].

Table 2: Apparent activation energy values for Pb and Pb-In alloys in 4 M H_2SO_4 solution at both peak (I) and passive region.

Pb or alloys	E_a (kJ·mol^{-1}) at Peak (I)	E_a (kJ·mol^{-1}) (in passive region at 1.2 V)
Pb	24.20	52.00
Alloy (I)	26.20	49.00
Alloy (II)	21.30	45.60
Alloy (III)	18.00	41.50
Alloy (IV)	16.60	26.11
Alloy (V)	15.00	22.00

3.2. Potentiostatic Measurements. In order to establish that the current density increases as a result of increasing In level in the alloy at two different applied potentials (peak I and passive region), potentiostatic measurements are examined of both Pb and its studied alloys. Figures 11 and 12 show the current-time transient curves of Pb and its alloys in the examined acid solution at 20°C. The results show clearly that the measured currents of the investigated electrodes at more positive potential (passive region) are significantly reduced (curves of Figure 12) in comparison with those obtained at more negative potential, peak I (curves of Figure 11). Visual observation indicated that the current density initially decreases gradually with time. This indicates that oxides of Pb and In formed on the surface of each electrode and the current flowing at this time may correspond to the film formation and repairing the film materials [30]. By comparing the current densities, it has been seen that immediately after switching on the applied potential (+1.2 V versus SCE), the value of current density of pure Pb is low compared to those of Pb-In alloys. Consequently, the current remains at a maximum value for alloy containing 15% In. The curves of Figure 11 (at peak I) exhibit that the steady state value of current density (except for alloy I) increases with increasing In content. These results clearly show that the addition of In to Pb aids in dissolution of the passive film and increases the reversibility of the anodic reaction [1]. This behaviour can be explained by the dissolution of In in H_2SO_4 solution leading to increase the ionic conductivity of the layer [24]. However, the data exhibited that the steady state value of current density in the case of alloy I (at peak potential) is lower than that of pure lead. These results support the potentiodynamic behaviour of the pure Pb and its studied alloys at the same applied potentials.

3.3. Chronopotentiometric Measurements. Chronopotentiometry at an anodic constant current density is utilized to get more information about the anodic behaviour of Pb and its investigated alloys in H_2SO_4 solution. Figures 13 and 14 show anodic potential/time transients of Pb and alloy V at different current densities (20–120 μA·cm^{-2}) and 20°C. The curves (except at 100 and 120 μA·cm^{-2} in the case of Pb only) exhibit active/passive transition at point B. The anodic potential remains almost constant along the arrest AB (the active dissolution region) and then suddenly rises at B to the inflection potential C and then tends to attain a

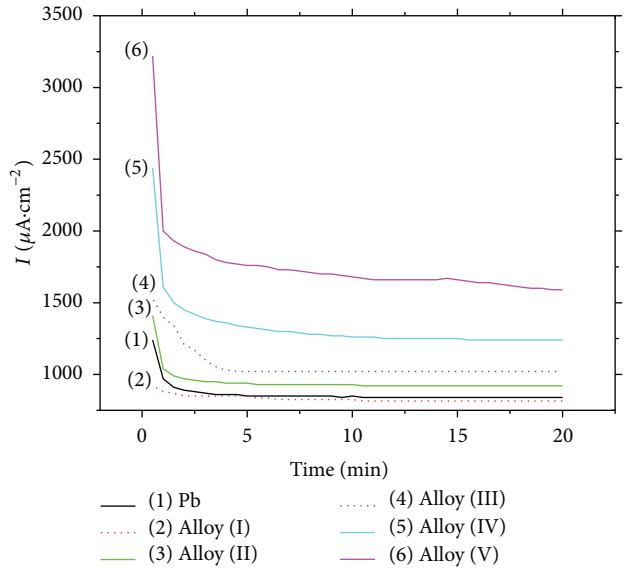

Figure 11: Potentiostatic transient's current versus time curves for Pb and its investigated alloys in 4 M H_2SO_4 solution at peak (I) potential and 20°C.

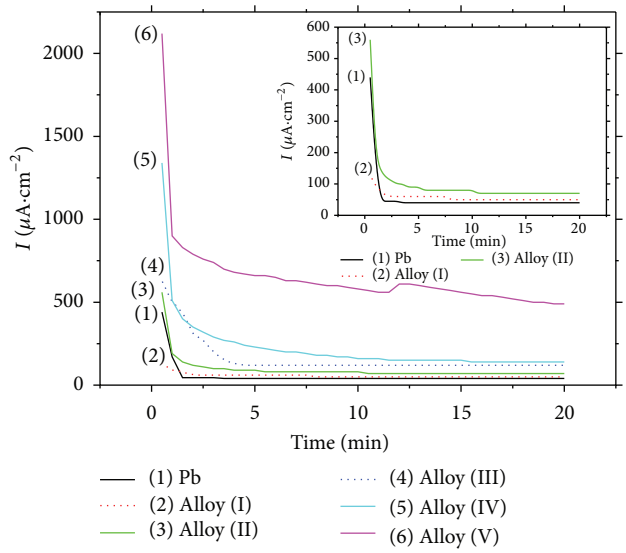

Figure 12: Potentiostatic transient's current versus time curves for Pb and its investigated alloys in 4 M H_2SO_4 solution at passive region (1.2 V) and 20°C.

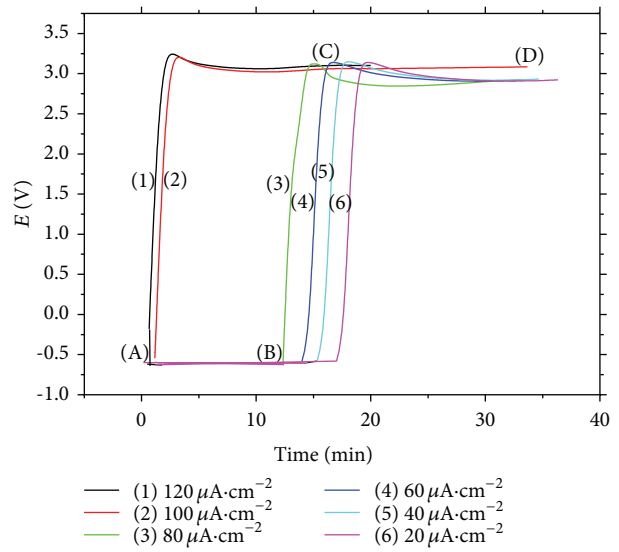

Figure 13: Anodic potential versus time curves for Pb in 4 M H_2SO_4 solution at different current densities and 20°C.

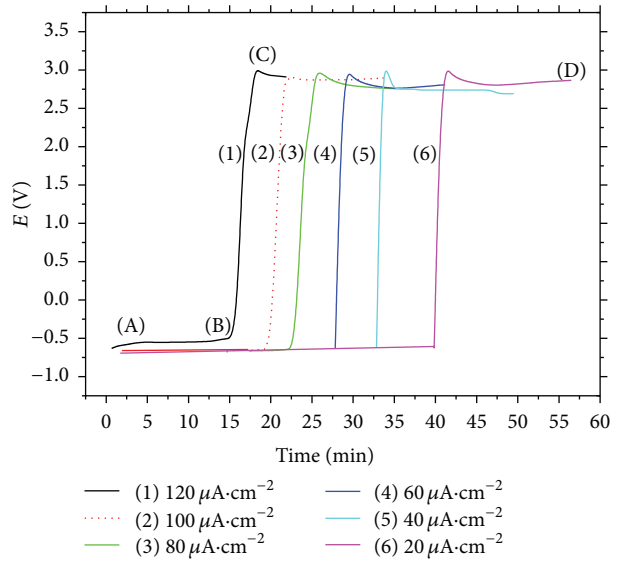

Figure 14: Anodic potential versus time curves for Pb-15 In alloy in 4 M H_2SO_4 solution at different current densities and 20°C.

steady state value (passive region). As mentioned above Pb dissolves in the active region as Pb^{2+} ion. The passivation may be due to the formation of a film on the anode surface containing $PbSO_4$ and PbO in the case of Pb and β-PbO_2 and In_2O_3 for alloy. Within the passivation region no oxygen evolution is observed, and the current flowing at this time may correspond to the film formation on the surface [16]. The time elapsed from the start of the test until the sudden rise in potential (B) is designated by passivation time ($t_{pass.}$). Subsequent to this process (BC), the passivation potential starts to slightly decrease before reaching steady state (CD region). This process may be attributed to the partial dissolution of oxides film. It is observed that the polarization curves (CD) deviated from linearity to reach steady state value. The potential deviation indicated a decrease in the film growth efficiency [31]. The value of $t_{pass.}$ decreases, while the steady state potentials in the passive region seem to be the same with increasing current density. This behaviour is related to the increase of the formation rate of the oxide with an increase of the applied current density. However, it is seen that immediately after switching on the applied higher current density (100 and 120 $\mu A \cdot cm^{-2}$ for pure Pb), the potential rises very rapidly and almost linearly to an inflection potential at C, denoting the occurrence of permanent passivation.

Below the inflection potential, the curve does not exhibit any potential arrest. Within this potential region, the flowing charge transfer reactions are thermodynamically possible:

$$Pb + SO_4^{2-} \longrightarrow PbSO_4 + 2e \quad (6)$$

and/or

$$Pb + H_2O \longrightarrow PbO + 2H^+ + 2e \quad (7)$$

It seems that under the prevailing conditions the rate of film formation is much faster than that of its dissolution. For this reason permanent passivation of the anode is attained very rapidly, especially if there are any oxides formed by atmospheric oxygen present on the Pb surface. The time elapsed from the start until the inflection point C is designated by $t_{pass.}$.

It is interesting to observe that the investigated alloys (Figure 14 as representative curves for alloy V) exhibit different behaviour to that observed in Figure 13 for pure Pb at higher current densities (100 and 120 $\mu A \cdot cm^{-2}$). This reveals that the anodic potential remains almost constant along arrest AB (the active dissolution region) for the alloys. This indicates that the dissolution rate of the passive film becomes higher than that of its formation at all applied current densities. This explanation can be accepted on the basis that addition of In to Pb retards the formation of both $PbSO_4$ and PbO (resistive film) on the surface, and consequently the film becomes more conducting with increasing In content.

Figure 15 shows the potential-time curves for Pb and its investigated alloys in the examined acid solution at 20 $\mu A \cdot cm^{-2}$ and 20°C. Careful inspection of these curves reveals that the addition of indium to Pb has no significant effect on the basic trends of the polarization curves. It is obvious that an increase in In content in the alloy enhances the value of $t_{pass.}$, and the steady state potential of the passive film is slightly shifted to less value. This indicates that the conductivity of the anodic film on the surface of lead alloy has been improved by increasing In content. It is in agreement with the potentiodynamic measurements. As mentioned above Pb and In dissolve in the active region as Pb^{2+} and $[In(OH)_4]^-$ ions according to the following reaction:

$$Pb + SO_4^{2-} \longrightarrow PbSO_4 + 2e \quad (8)$$

However, the formation of $PbSO_4$ on the alloy surface decreases with In level in the alloy and may be completely prevented at higher In content (15% In). Therefore, dissolution of $PbSO_4$ becomes easier as the following:

$$PbSO_4 \longleftrightarrow Pb^{2+} + SO_4^{2-} \quad (9)$$

At the same time during the anodic polarization under the imposed current density on the surface, indium in the alloy dissolves as $In[(OH)_4]^-$ according to the following:

$$In + 2H_2O \longrightarrow InOOH + 3H^+ + 3e \quad (10)$$

$$InOOH + 2H_2O \longrightarrow [In(OH)_4]^- + H^+ \quad (11)$$

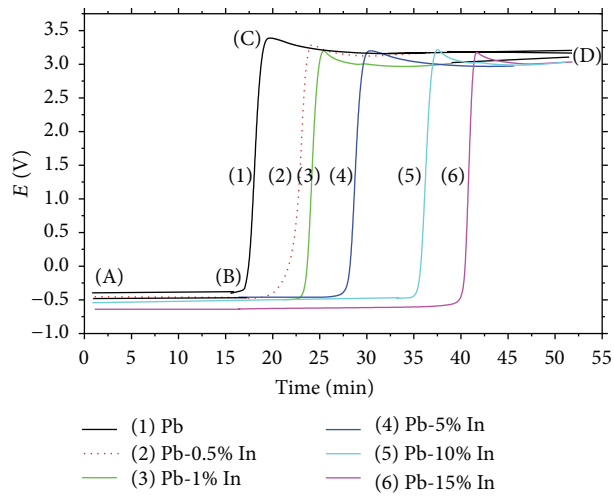

Figure 15: Comparison between anodic potential versus time curves for Pb and Pb-In alloys in 4 M H_2SO_4 solution at 20 $\mu A \cdot cm^{-2}$ and 20°C.

Accordingly, the anode dissolves continuously as Pb^{2+} and $[In(OH)_4]^-$ without passivation. Then, the anode potential rises very rapidly at B (active-passive transition) to the inflection potential C. This behaviour can be attributed to the oxidation of Pb^{2+} to β-PbO_2 as the following [32]:

$$Pb^{2+} + 2H_2O \longrightarrow \beta\text{-}PbO_2 + 4H^+ + 2e \quad (12)$$

As mentioned before, the oxidation rate of $PbSO_4$ increased with increasing In content. In addition, the transformation of a hydrated and ionically conducting indium oxide layer into a more stable crystalline and electronically conducting type of oxide occurs with loss of water [26]:

$$2InOOH \longrightarrow In_2O_3 + H_2O \quad (13)$$

When the formation rate of oxides (PbO_2 and In_2O_3) exceeds its dissolution rate, the potential rises suddenly at B to the inflection C.

Comparison between these curves shows that the passivation time ($t_{pass.}$) increases with increasing In content. It is evident that an increase in In content increases the time required to achieve passivation ($t_{pass.}$). This behavior can be attributed to the presence of In which retards the formation of PbO and facilitates the oxidation of $PbSO_4$ to PbO_2. It can be clearly shown that the tendency of the alloys towards passivity decreases with increasing In content. Accordingly, the investigated alloys required more time to reach passivation compared with that of pure Pb. Consequently, the data exhibited that the time required reaching the electrode surface to the passivation decreases in the following order:

$$\text{alloy V} > \text{alloy IV} > \text{alloy III} > \text{alloy II} > \text{alloy I} > \text{Pb} \quad (14)$$

Therefore, it can be clearly seen that the tendency of the alloys to passivity is delayed with an increase in indium content.

The relation between the current density and passivation time is best represented by plotting these two variables on

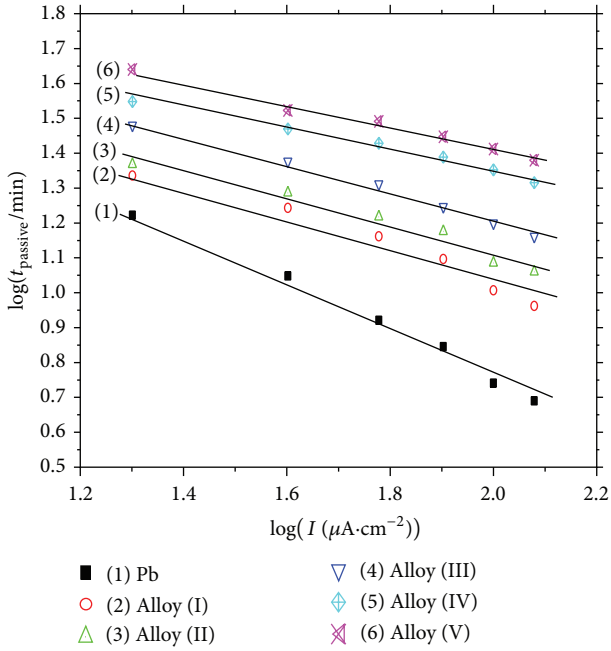

Figure 16: Linear dependence of log $t_{pass.}$ versus log I of Pb and Pb-In alloys in 4 M H_2SO_4 solution and at 20°C.

a double logarithmic scale (Figure 16), where a straight line relation is obtained and is satisfactorily represented by the equation

$$\log t_{pass.} = a - b \log I \quad (15)$$

where a and b are constants. A similar relation has been derived by Müller [33] who considered the formation of a layer leading to the passivation of the metal electrode in a solution saturated with the reaction product. These results together with those obtained by both potentiodynamic and potentiostatic techniques assume that the electron conductivity of the passivation layer increases with the indium level in the lead alloy. Therefore, one of the effects of In is to decrease the thickness of both $PbSO_4$ and PbO layers, during both the charge and discharge of Pb-acid batteries. The standard electrode potential of electrochemical reaction is shown in Table 3.

3.4. Cyclic Voltammetric Measurements. Figure 17 represents the cyclic voltammograms of Pb and some investigated Pb-In alloys in 4 M H_2SO_4 solution at scan rate 10 mV s^{-1}. Each electrode was kept for 60 s at −1.5 V versus SCE, and then the potential was swept from −1.2 V up to +1.5 V. On positive going sweep, the active dissolution region involves one anodic peak (A) in the case of Pb, corresponding to the formation of a $PbSO_4$ layer. While, with continuous the sweeping potential to more positive direction, PbO is formed under $PbSO_4$ perm-selective membrane permeable [34]. But, on the negative-going scan, a small peak (C_I) appears at about −0.7 V, corresponding to the reduction of the PbO formed underneath the passive layer of $PbSO_4$. In addition, at more negative potential (C_{II}), $PbSO_4$ is reduced to Pb metal.

Table 3: Standard electrode potential of electrochemical reaction formula.

Electrochemical reaction	Standard potential versus SHE, V
$Pb \rightarrow Pb^{2+} + 2e$	−0.13
$PbSO_4 + 2H_2O \rightarrow \beta\text{-}PbO_2 + H_2SO_4 + 2H^+ + 2e$	+1.69
$Pb + SO_4^{2-} \rightarrow PbSO_4 + 2e$	−0.36
$Pb^{2+} + 2H_2O \rightarrow \beta\text{-}PbO_2 + 4H^+ + 2e$	+1.12
$In \rightarrow In^+ + e$	−0.23
$2In + 3H_2O \rightarrow In_2O_3 + 6H^+ + 6e^-$	−0.431

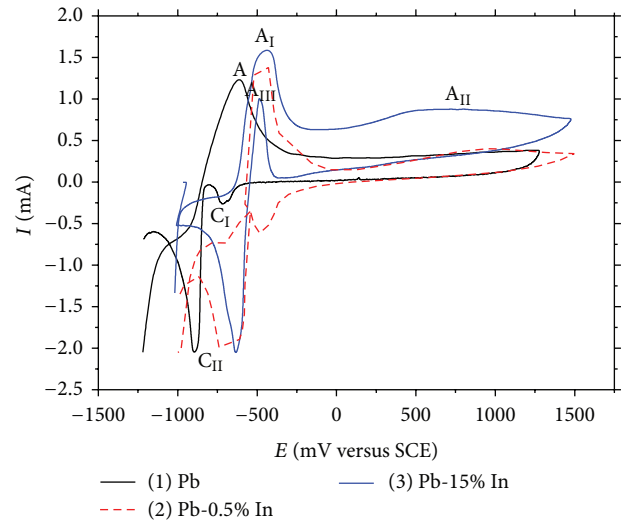

Figure 17: Cyclic voltammograms of Pb, Pb-0.5% In, and Pb-15% In alloys in 4 M H_2SO_4 solution at scan rate 10 mV s^{-1}.

However, in the case of Pb-In alloys two anodic peaks A_I and A_{II} are formed. Obviously the anodic oxidation peaks move to more positive potential, and the current of peak increases gradually with increasing In content. The first peak may be due to oxidation of Pb to $PbSO_4$ or PbO_2, while the small broad peak (A_{II}) may correspond to the dissolution of Pb-In phase [8]. On the other hand, the obtained behaviour of cyclic voltammograms of alloys II to IV (not represented here) is similar to that of alloy I.

By comparing between cyclic voltammograms of pure Pb, Pb-0.5% In, and Pb-15% In alloys (Figure 17), it is observed that the anodic oxidation peak (A_I) shifts to more positive potential, and the peak current (A_I) of the two mentioned alloys is higher compared to that of pure Pb. This behavior can be ascribed to that alloying In decreases the thickness of the passivation layer on the alloy surface. On the other hand, the conductivity of the passivation layer is increased as the In level increases in the alloy. It is interesting to observe that by increasing In content (up to 15%), the peak related to the reduction of PbO at negative back scan is not observed as in both pure lead and the lower In content in the alloy (0.5% to 10% In). Moreover, the third peak (A_{III}) appears at the reverse scan (at potential close to −0.5 V), but the peak

current is observed in the positive anodic direction in the case of alloy V (15% In). This criterion is very important, and similar behavior has been reported by Abd El Rehim et al. [16] for anodic dissolution of tin in maleic acid solution. This peak may be attributed to the oxidation of uncombined In at higher In content only. However, In can be oxidized to In^+ species at certain potential (−0.5 V). Chung and Lee [35] studied the electrochemical behavior of In in acidic solution. They detected In^+ species formed during the anodic dissolution of indium at −0.5 V. The present results suggest that the anodic oxidation of In is more difficult for Pb alloy containing In than that of pure In electrode. This explanation is in accordance with that previously mentioned by Li et al. [36] for anodic oxidation of Pb alloy in H_3PO_4 solution. Accordingly, one can conclude that the higher In content (15% In) prevents the formation of PbO on the alloy surface, and its absence is confirmed by XRD, EDX, and SEM analysis.

3.5. Composition and Properties of Anodic Film. In order to investigate the type and nature of passive film formed on the surface of both Pb and its studied alloys, X-ray diffraction, EDX, and SEM are examined. The composition of the passive film formed on the surfaces of the studied electrodes, after the anodic potentiostatic polarization treatment in H_2SO_4 solution for 20 min at different formation potentials, was studied. Each passive electrode was withdrawn carefully, washed with doubly distilled water, dried, and finally examined.

3.5.1. X-Ray Diffraction. The data for the composition nature of passive film formed at peak potential I of Pb (Figure 18) confirm the existence of Pb, PbO, Pb_3O_4, and $PbSO_4$ constituents. These results indicate that the peak potential of Pb is related to the formation of PbO and $PbSO_4$, in addition to Pb_3O_4 constituent. X-ray diffraction data (passive region) exhibit that the surface contains very small amounts of PbO and β-PbO_2 and large amounts of $PbSO_4$. This indicates that $PbSO_4$ is more predominant and PbO seems to be very small in the passive region. X-ray data for alloy I (0.5% In) at peak potential (Figure 19) indicate that the surface contains large amounts of Pb, β-PbO_2, and In_2O_3 and small amounts of PbO and $PbSO_4$. This exhibits that the presence of In (0.5%) in the alloy firstly retards the oxidation of Pb to PbO, and accordingly the formation of PbO on the surface is significantly reduced. The data for the same studied alloy in the passive region (Figure 20) reveal that the surface contains Pb, β-PbO_2, and $PbSO_4$ and small amounts of In_2O_3. Comparison between X-ray data for the presence of both PbO and $PbSO_4$ on the surfaces of Pb and Pb-0.5% In alloy reveals small amounts of $PbSO_4$ and PbO of alloy compared with the large amounts in the case of pure Pb.

X-ray data in Figure 21 for alloy V (15% In) at peak potential reveal that the surface contains a large amount of Pb and small amounts of β-PbO_2 and In_2O_3, while $PbSO_4$ completely disappeared. This observation supports our suggestion that addition of In to Pb, particularly at high In content, prevents the formation of $PbSO_4$ through its oxidation to β-PbO_2. On the other hand, the data (XRD) for the mentioned alloy, but in the passive region (not represented here), reveal that the

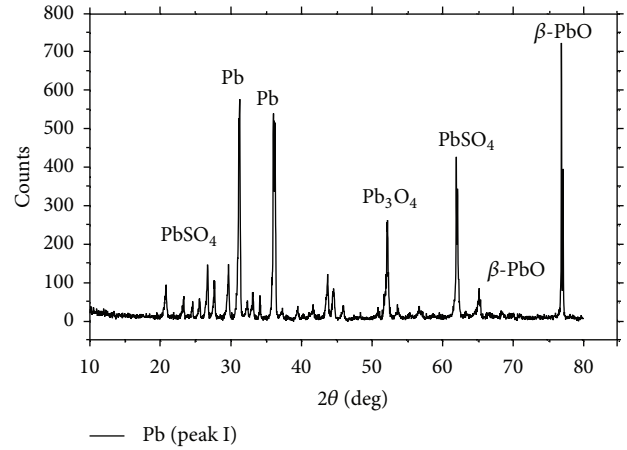

Figure 18: X-ray diffraction analysis for the passive film on Pb surface formed anodically in 4 M H_2SO_4 solution at peak potential and at 20°C.

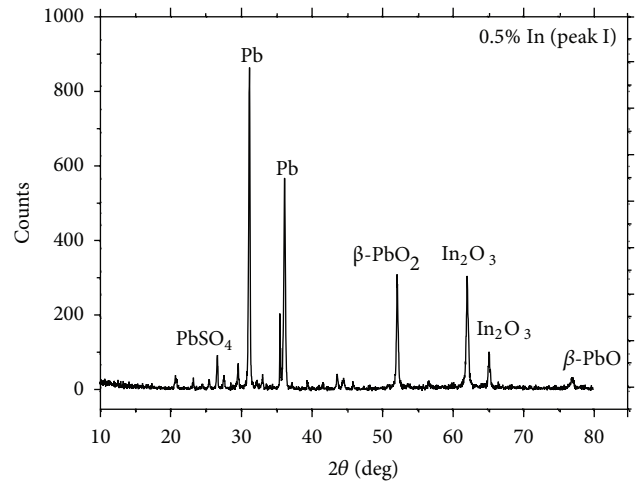

Figure 19: X-ray diffraction analysis for the passive film on Pb-0.5 In alloy surface formed anodically in 4 M H_2SO_4 solution at peak potential and at 20°C.

surface is covered also by β-PbO_2 and In_2O_3. This indicates that β-PbO_2 and In_2O_3 prevail at high positive potentials. This result clearly shows that the formation of In_2O_3 with β-PbO_2 in the passive region aids in the dissolution of the passive film and consequently increases the passivation current density. The X-ray data support that alloying with indium improves the electronic conduction of the passive layers, due to the presence of indium in the film, in an ionic or oxide form.

3.5.2. EDX Spectroscopy and SEM Micrographs. Figures 22(a)–22(c) represent an EDX spectroscopy for Pb metal, Pb-0.5% In, and Pb-15% In alloys surfaces exposed to passive film formed anodically at peak I potential in the examined acid solution. Figure 22(a) exhibits the characteristic peaks which are related to Pb, S, and O. This indicates that the corrosion product on pure Pb surface is $PbSO_4$ and PbO. However,

Table 4: Surface element content (atomic %) of Pb, alloy I, and alloy V at both peak potential and passive region using EDX analysis.

Electrode	At peak potential			At passive region		
	Pb	Alloy I	Alloy V	Pb	Alloy I	Alloy V
Element		Element (atomic %)			Element (atomic %)	
O	57.86	71.97	85.44	55.28	60.45	84.23
S	19.72	14.0	—	10.87	9.50	—
In	—	5.12	9.45	—	4.28	8.23
Pb	22.42	8.91	5.11	33.85	25.77	7.54

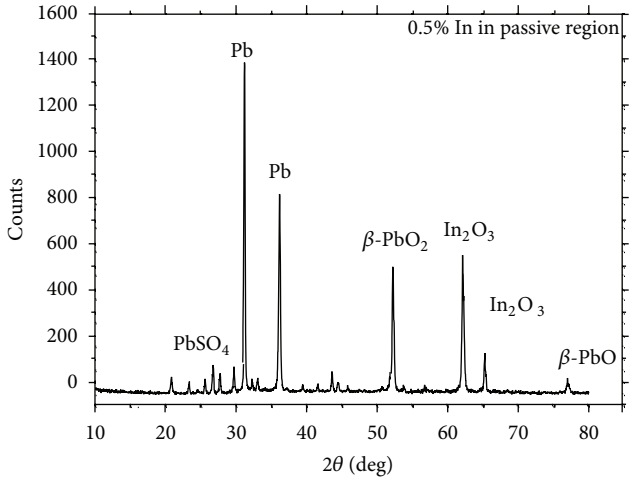

Figure 20: X-ray diffraction analysis for the passive film on Pb-0.5 In alloy surface formed anodically in 4 M H_2SO_4 solution at passive potential and at 20°C.

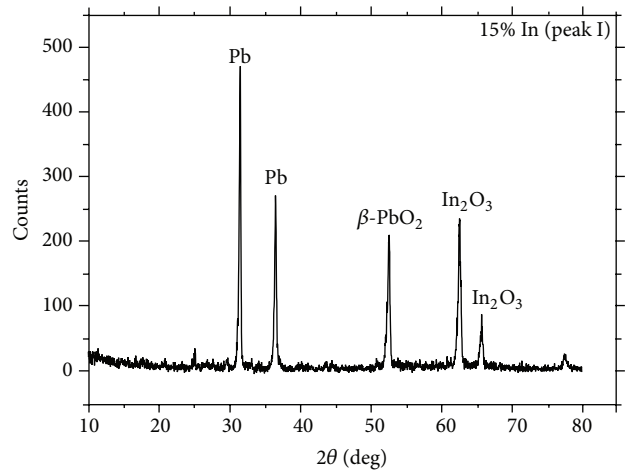

Figure 21: X-ray diffraction analysis for the passive film on Pb-15 In alloy surface formed anodically in 4 M H_2SO_4 solution at peak potential and at 20°C.

the data in Figure 22(b) show additional characteristic peaks of In element, and the peaks heights of Pb and S are lower than those observed in the case of pure Pb. This result proved that the amount of $PbSO_4$ is decreased, due to the presence of In in the alloy. Figure 22(c) exhibits peaks of Pb, In, and O elements only. This result indicates that the corrosion product on the surface of Pb-15% In alloy is β-PbO_2 and In_2O_3. The absence of peaks related to S element for the mentioned alloy, indicating that the formation of $PbSO_4$ on the Pb-15% In alloy surface is completely prevented. Similar behavior is obtained for the same investigated metal and its alloys in the passive region (Figure 23). The data of surface element content (atomic %) of Pb, alloy I and alloy V at both peak potential and passive region using EDX analysis, are shown in Table 4. It is very interesting to observe that the S element disappears in the case of alloy V (15% In). This further confirms that $PbSO_4$ does not form at higher In content, and this result is consistent with that of XRD analysis. It can be probably explained by the fact that a large amount of In element has to be present on the surface of the alloy, to prevent the formation of $PbSO_4$.

Figures 24(a)–24(c) show the SEM photographs of Pb, Pb-0.5% In, and Pb-15% In alloys, respectively, at peak I potential. The data in Figure 24(a) infer that the surface exhibits two layers of the corrosion film. The quantity of the upper layer is denser and covers most of the surface. The particles of the upper layer become loosely bound to the Pb surface. The particles in the underneath layer are very low, and much larger in size. This result suggests that the upper layer is $PbSO_4$, and the underneath layer is PbO. However, the photograph of Pb-0.5% In alloy treated under the same conditions given in Figure 24(b) recognized that the quantity of $PbSO_4$ at the upper layer is less than that observed in Figure 24(a), and the vacancies between particles become wider so that the underneath layer appears easily through them. In addition, the amount of particles in the underneath layer is greater compared with that of the same layer formed in the case of pure Pb. This indicates that the presence of In as a minor alloying element retards the formation of $PbSO_4$ and enhances the formation of β-PbO_2. Figure 24(c) shows two layers on the alloy surface. It is observed that the crystals of upper layer exhibit different shapes, that is, like the sticks and are loosely distributed on the surface with different orientations. The second layer seems to exist below the upper layer and is not compact and porous. These observations are in agreement with the data of X-ray diffraction that the upper layer may be related to In_2O_3 and $In(OH)_3$, while the underneath layer contains lead oxides. It is very interesting to observe that $PbSO_4$ completely disappeared on the surface of alloy V (15% In) compared with that observed in both Pb and Pb-0.5% In alloy.

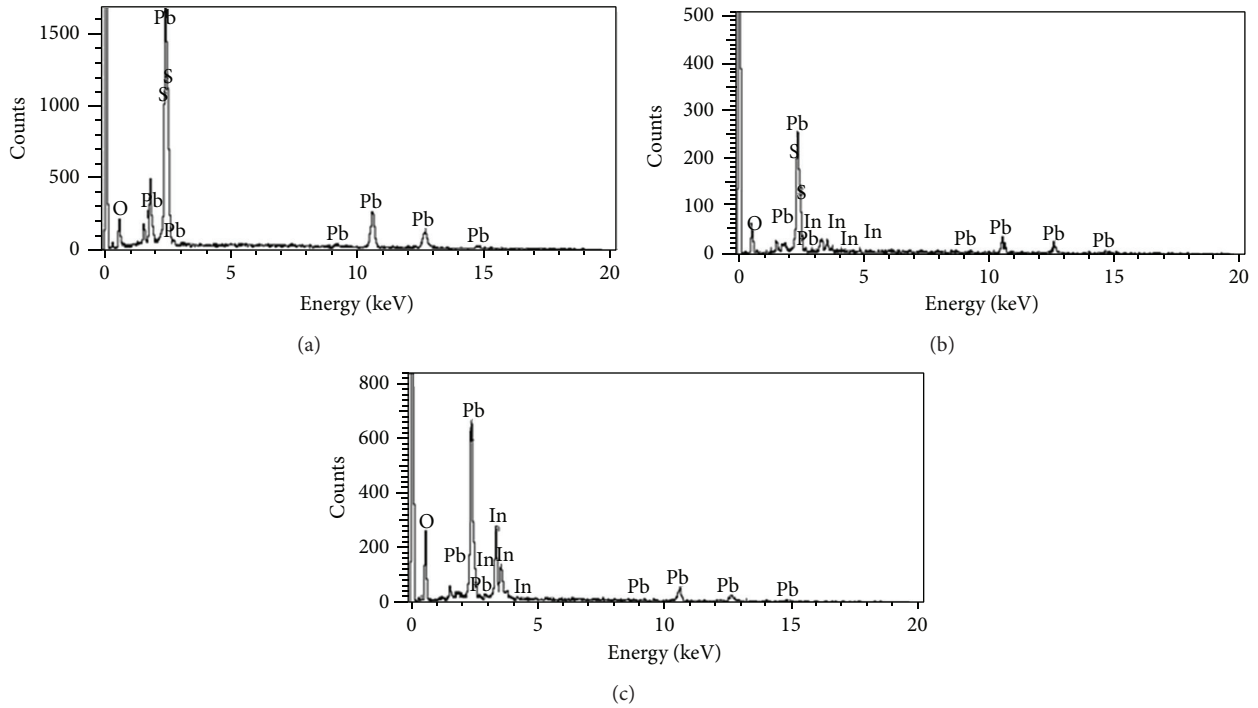

Figure 22: EDX spectrum for the passive film on (a) Pb, (b) Pb-0.5 In alloy, and (c) Pb-15 In alloy surface formed anodically in 4 M H_2SO_4 solution at peak potential and at 20°C.

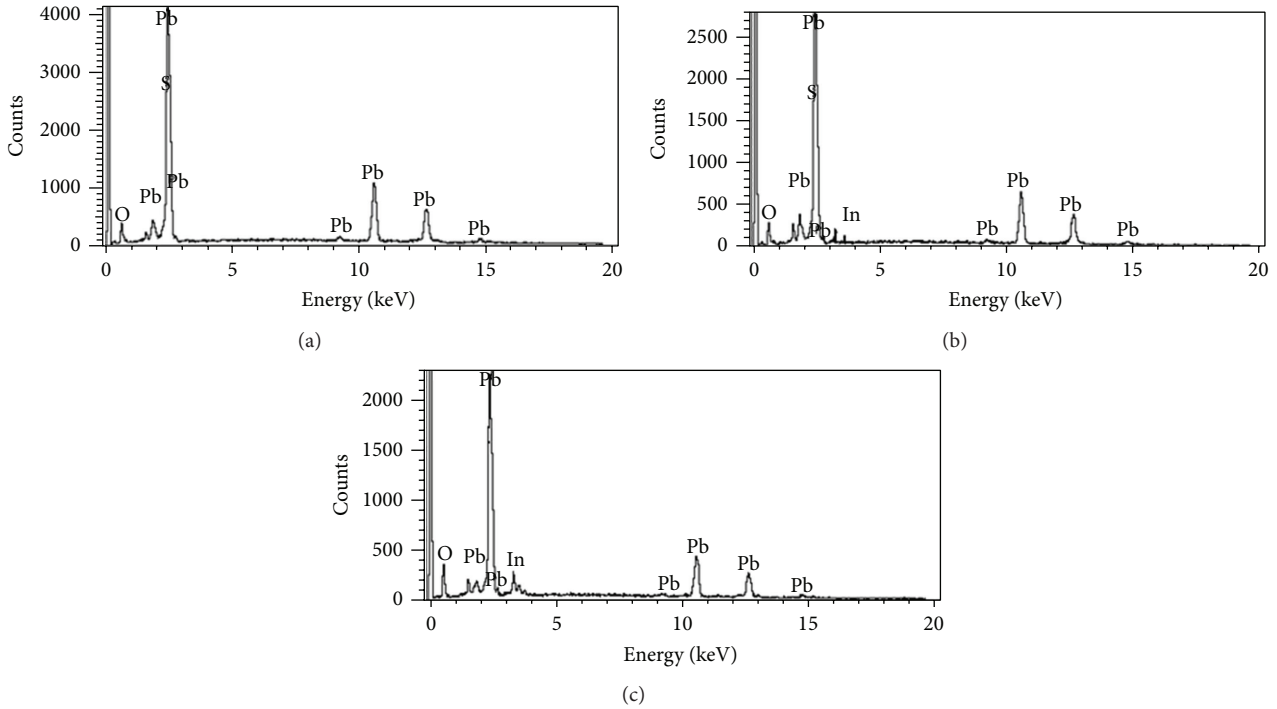

Figure 23: EDX spectrum for the passive film on (a) Pb, (b) Pb-0.5 In alloy, and (c) Pb-15 In alloy surface in 4 M H_2SO_4 solution at passive region (1.2 V versus SCE) and at 20°C.

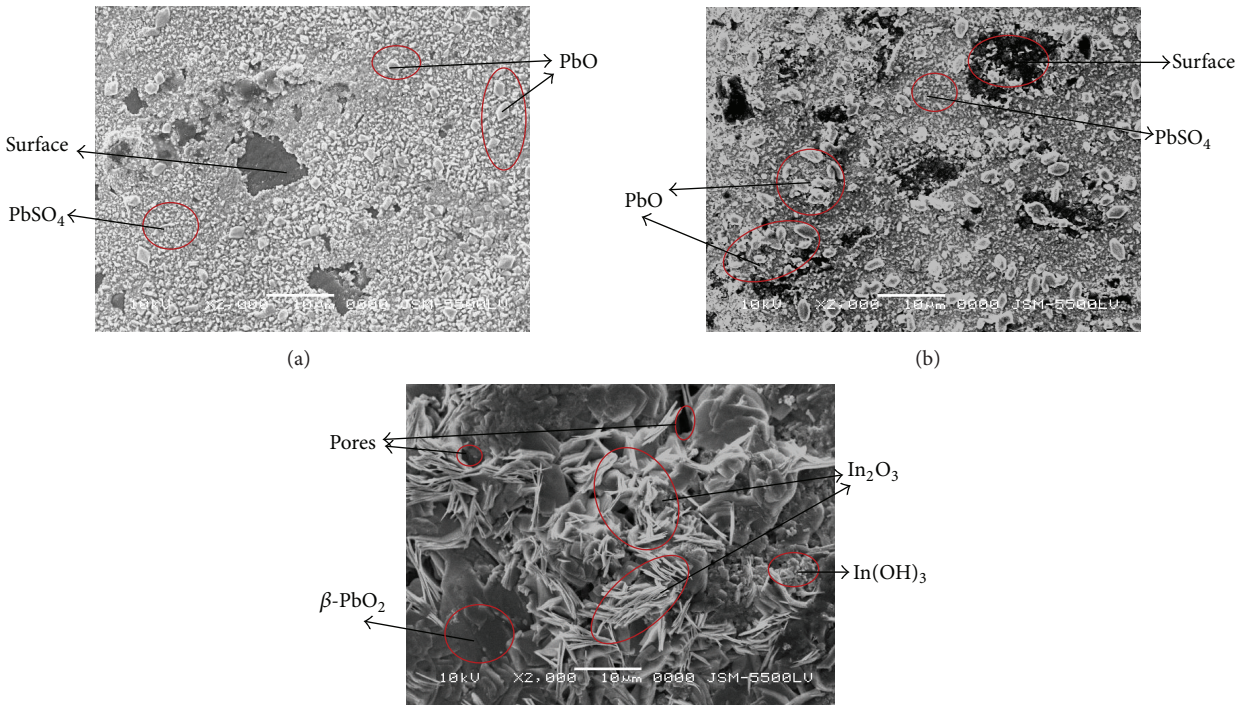

FIGURE 24: SEM photographs of passive film on (a) Pb, (b) Pb-0.5 In alloy, and (c) Pb-15 In alloy surface formed anodically in 4 M H_2SO_4 solution at peak potential and at 20°C.

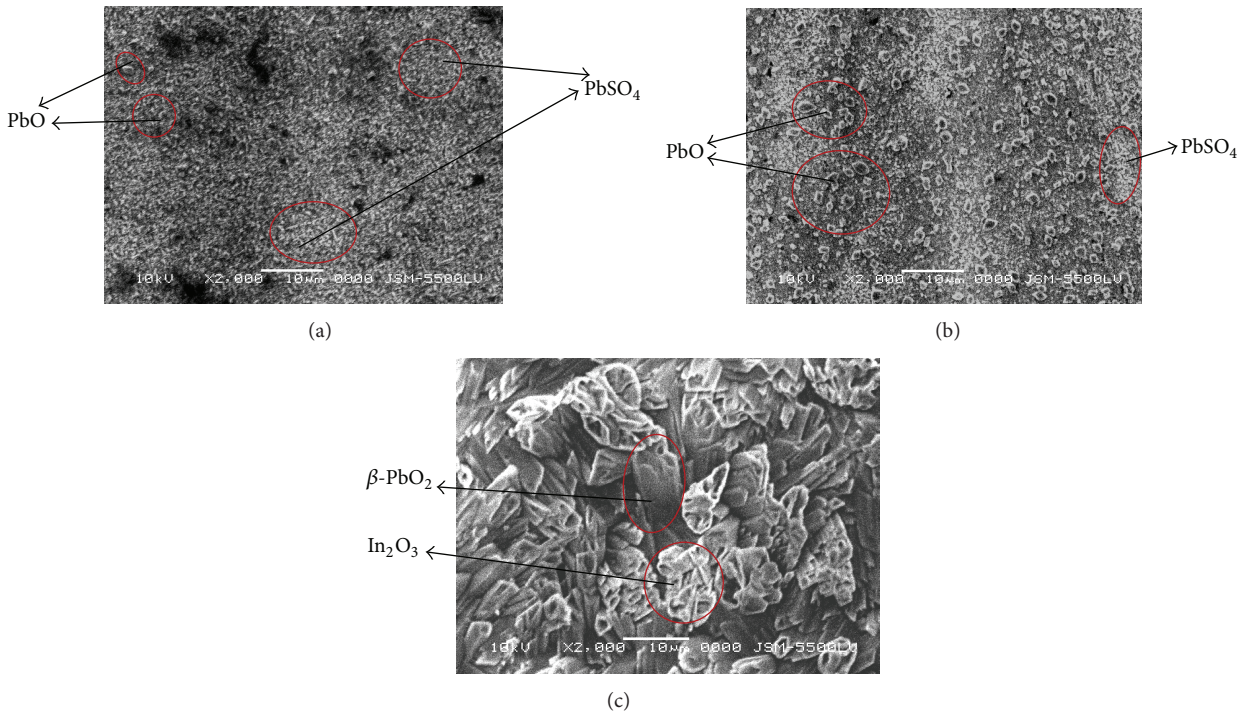

FIGURE 25: SEM photographs of passive film on (a) Pb, (b) Pb-0.5 In alloy, and (c) Pb-15 In alloy surface formed anodically in 4 M H_2SO_4 solution at passive region (1.2 V versus SCE) and at 20°C.

Figures 25(a), 25(b), and 25(c) show the micrographs of the anodic passive film formed potentiostatically on the surfaces of the above-mentioned electrodes at 1.2 V versus SCE. It would be seen that the surface of pure Pb seems to be completely covered by the passive film so that the underneath layer can not be seen. Figure 25(b) shows two layers; the quantity of the upper layer ($PbSO_4$) is less than that observed in Figure 25(a), while the quantity of oxide patches in the underneath layer is greater than that observed for pure Pb. Figure 25(c) shows two layers on the surface. The upper layer is due to In_2O_3 formation, but the underneath layer belongs to β-PbO_2. Generally, the passive films at more positive potential (1.2 V versus SCE) are denser than those at peak potential. These observations are confirmed by XRD and EDX and are in good agreement with electrochemical measurements. Based on these interpretations, minor In alloying with Pb reduces the rate of corrosion and promotes the formation of a conductive corrosion film. Therefore, nonconducting layer at the grid/active material can be eliminated and recharge of the battery will be improved.

4. Conclusions

In this paper the effect of indium content on both anodic dissolution and passivation behavior of Pb-In alloy in H_2SO_4 solution was investigated by different techniques. Several conclusions can be withdrawn from this investigation.

(1) The potentiodynamic and chronopotentiometric curves show that the anodic behaviour of all investigated electrodes exhibits active/passive transition. The active dissolution (except for alloy I) and passive currents increase with increasing both In content and temperature.

(2) Chronopotentiometric measurements exhibit that the passivation time increases with increasing In content. Therefore, it can be clearly seen that the tendency of the alloy to passivity is delayed with increase in indium content. Therefore, one of the effects of In is to decrease the thickness of both $PbSO_4$ and PbO layers, during both the charge and discharge of Pb-acid batteries.

(3) The values of activation energy (E_a) in the passivation region decrease gradually with increasing In content and reaches its minimum value in the case of alloy V. This indicates that the passive film formed on Pb-In alloy with In content exhibits good electronic conductivity, while the passive film formed on pure lead is more resistive.

(4) Cyclic voltammetric measurements show that at higher In content (15% In), the peak related to the reduction of PbO at negative back scan is not observed compared with that of both pure Pb and each alloy having lower In content. This indicates that the presence of high In content prevents the oxidation of Pb to PbO on the alloy surface. Moreover, third oxidation peak (A_{III}) is observed at the reverse scan. This peak may be attributed to the oxidation of uncombined In at higher In content only.

(5) XRD, EDX, and SEM results reveal that the formation of both $PbSO_4$ and PbO on the surface decreases gradually with increasing In level in the alloy and is completely prevented at higher In content (15% In). Accordingly, the electronic resistance of the passive layer is decreased, due to the presence of In in the film, in an ionic or oxide form.

(6) Based on these interpretations, minor In alloying with Pb reduces the rate of corrosion and promotes the formation of a conductive corrosion film. Therefore, nonconducting layer at the grid/active material can be eliminated and recharge of the battery will be improved.

Conflict of Interests

The authors declare that there is no conflict of interests regarding the publication of this paper.

References

[1] D. Slavkov, B. S. Haran, B. N. Popov, and F. Fleming, "Effect of Sn and Ca doping on the corrosion of Pb anodes in lead acid batteries," *Journal of Power Sources*, vol. 112, no. 1, pp. 199–208, 2002.

[2] B. Culpin, A. F. Hollenkamp, and D. A. J. Rand, "The effect of tin on the performance of positive plates in lead/acid batteries," *Journal of Power Sources*, vol. 38, no. 1-2, pp. 63–74, 1992.

[3] R. F. Nelson and D. M. Wisdom, "Pure lead and the tin effect in deep-cycling lead/acid battery applications," *Journal of Power Sources*, vol. 33, no. 1–4, pp. 165–185, 1991.

[4] K. R. Bullock and M. A. Butler, "Corrosion of lead in sulfuric acid at high potentials," *Journal of the Electrochemical Society*, vol. 133, no. 6, pp. 1085–1090, 1986.

[5] D. Pavlov and R. Popova, "Mechanism of passivation processes of the lead sulphate electrode," *Electrochimica Acta*, vol. 15, no. 9, pp. 1483–1491, 1970.

[6] J. S. Buchanan, N. P. Freestone, and L. M. Peter, "A photoelectrochemical study of the anodic oxidation of lead in alkaline solution," *Journal of Electroanalytical Chemistry*, vol. 182, no. 2, pp. 383–398, 1985.

[7] J. S. Buchanan and L. M. Peter, "Photocurrent spectroscopy of the lead electrode in sulphuric acid," *Electrochimica Acta*, vol. 33, no. 1, pp. 127–136, 1988.

[8] I. Petersson and E. Ahlberg, "Oxidation of electrodeposited lead-tin alloys in 5 M H_2SO_4," *Journal of Power Sources*, vol. 91, no. 2, pp. 143–149, 2000.

[9] P. Ruetschi, "Ion selectivity and diffusion potentials in corrosion layers: films on Pb in H_2SO_4," *Journal of the Electrochemical Society*, vol. 120, no. 3, pp. 331–336, 1973.

[10] R. Miraglio, L. Albert, A. El Ghachcham, J. Steinmetz, and J. P. Hilger, "Passivation and corrosion phenomena on lead-calcium-tin alloys of lead/acid battery positive electrodes," *Journal of Power Sources*, vol. 53, no. 1, pp. 53–61, 1995.

[11] G. H. Brilmyer, "Photoelectrochemical characterization of lead corrosion films," in *Advances in Lead-Acid Batteries*, K. Bullock

and D. Pavlov, Eds., vol. 84-14 of *Proceedings of the Electrochemical Society*, pp. 142–153, Electrochemical Society, Pennington, NJ, USA, 1984.

[12] H. Döring, J. Garche, H. Dietz, and K. Wiesener, "Currentless passivation of the PbO_2 electrode with respect to the influence of tin," *Journal of Power Sources*, vol. 30, no. 1–4, pp. 41–45, 1990.

[13] D. Pavlov, B. Monakhov, M. Maja, and N. Penazzi, "Mechanism of action of Sn on the passivation phenomena in the lead-acid battery positive plate (Sn-free effect)," *Journal of the Electrochemical Society*, vol. 136, no. 1, pp. 27–33, 1989.

[14] P. Mattesco, N. Bui, P. Simon, and L. Albert, "Effect of polarisation mode, time and potential on the properties of the passive layer on lead-tin alloys," *Journal of Power Sources*, vol. 64, no. 1-2, pp. 21–27, 1997.

[15] A. El-Sayed, A. M. Shaker, and H. Gad El-Kareem, "Anodic behaviour of antimony and antimony-tin alloys in alkaline solutions," *Bulletin of the Chemical Society of Japan*, vol. 76, no. 8, pp. 1527–1535, 2003.

[16] S. S. Abd El Rehim, H. H. Hassan, and N. F. Mohamed, "Anodic behaviour of tin in maleic acid solution and the effect of some inorganic inhibitors," *Corrosion Science*, vol. 46, no. 5, pp. 1071–1082, 2004.

[17] A.-R. El-Sayed, H. S. Mohran, and H. M. Abd El-Lateef, "Effect of minor nickel alloying with zinc on the electrochemical and corrosion behavior of zinc in alkaline solution," *Journal of Power Sources*, vol. 195, no. 19, pp. 6924–6936, 2010.

[18] W. R. Osório, L. C. Peixoto, and A. Garcia, "Electrochemical corrosion of Pb-1 wt% Sn and Pb-2.5 wt% Sn alloys for lead-acid battery applications," *Journal of Power Sources*, vol. 194, no. 2, pp. 1120–1127, 2009.

[19] L. C. Peixoto, W. R. Osório, and A. Garcia, "Microstructure and electrochemical corrosion behavior of a Pb-1 wt%Sn alloy for lead-acid battery components," *Journal of Power Sources*, vol. 192, no. 2, pp. 724–729, 2009.

[20] H. Liang and Z. Wang, "Effect of indium addition on the electrochemical behavior of zinc electrodes in concentrated alkaline solutions," *Advanced Materials Research*, vol. 721, pp. 95–104, 2013.

[21] I. Mukhopadhyay, S. Ghosh, and M. Sharon, "Anodic oxidation of Pb—in alloys in alkaline solution: effect of in on electrochemical and photoelectrochemical behaviour of lead oxide," *Solar Energy Materials and Solar Cells*, vol. 53, no. 1-2, pp. 83–94, 1998.

[22] E. N. Codaro and J. R. Vilche, "A kinetic study of the electroformation of PbO_2 on Pb electrodes in sulphuric acid solutions," *Electrochimica Acta*, vol. 42, no. 4, pp. 549–555, 1997.

[23] J. Xu, X. Liu, X. Li, E. Barbero, and C. Dong, "Effect of Sn concentration on the corrosion resistance of Pb-Sn alloys in H_2SO_4 solution," *Journal of Power Sources*, vol. 155, no. 2, pp. 420–427, 2006.

[24] N. Bui, P. Mattesco, P. Simon, and N. Pébère, "Fundamental research on the role of alloying tin as a means to eliminate the passivation phenomena in lead/acid batteries," *Journal of Power Sources*, vol. 73, no. 1, pp. 30–35, 1998.

[25] M. Bojinov, K. Salmi, and G. Sundholm, "Influence of tin on the anodic behaviour of lead in sulphuric acid solutions-I. Voltammetric, photoelectrochemical and AC impedance measurements on a Pb-10%Sn alloy," *Electrochimica Acta*, vol. 39, no. 5, pp. 719–726, 1994.

[26] A.-R. El-Sayed, H. S. Mohran, and H. M. Abd El-Lateef, "Anodic behavior of tin, indium, and tin-indium alloys in oxalic acid solution," *Journal of Solid State Electrochemistry*, vol. 13, no. 8, pp. 1279–1290, 2009.

[27] S. S. Abdel Rehim, S. M. Sayyah, and M. M. El Deeb, "Corrosion of tin in citric acid solution and the effect of some inorganic anions," *Materials Chemistry and Physics*, vol. 80, no. 3, pp. 696–703, 2003.

[28] A.-R. El-Sayed, H. S. Mohran, and H. M. Abd El-Lateef, "Potentiodynamic studies on anodic dissolution and passivation of tin, indium and tin-indium alloys in some fruit acids solutions," *Corrosion Science*, vol. 51, no. 11, pp. 2675–2684, 2009.

[29] P. Simon, N. Bui, N. Pebere, F. Dabosi, and L. Albert, "Characterization by electrochemical impedance spectroscopy of passive layers formed on lead-tin alloys, in tetraborate and sulfuric acid solutions," *Journal of Power Sources*, vol. 55, no. 1, pp. 63–71, 1995.

[30] A.-R. El-Sayed, H. S. Mohran, and H. M. Abd El-Lateef, "Inhibitive action of ferricyanide complex anion on both corrosion and passivation of zinc and zinc-nickel alloy in the alkaline solution," *Journal of Power Sources*, vol. 196, no. 15, pp. 6573–6582, 2011.

[31] E. E. Abd El Aal, "Kinetic studies of zinc passivation in borate solutions under different conditions," *Corrosion*, vol. 55, no. 6, pp. 582–589, 1999.

[32] D. G. Li, D. R. Chen, J. D. Wang, and H. S. Chen, "Influences of temperature, H_2SO_4 concentration and Sn content on corrosion behaviors of PbSn alloy in sulfuric acid solution," *Journal of Power Sources*, vol. 196, no. 20, pp. 8789–8801, 2011.

[33] W. J. Müller, "On the passivity of metals," *Transactions of the Faraday Society*, vol. 27, pp. 737–751, 1931.

[34] S. Brinić, M. Metikoš-Huković, and R. Babic, "Characterization of anodic films on lead and lead alloys by impedance spectroscopy," *Journal of Power Sources*, vol. 55, no. 1, pp. 19–24, 1995.

[35] Y. Chung and C. W. Lee, "Electrochemical behaviors of Indium," *Journal of Electrochemical Science and Technology*, vol. 3, no. 1, pp. 1–13, 2012.

[36] S. Li, H. Y. Chen, M. C. Tang et al., "Electrochemical behavior of lead alloys in sulfuric and phosphoric acid electrolyte," *Journal of Power Sources*, vol. 158, no. 2, pp. 914–919, 2006.